

# EUROPHYSICS LETTERS

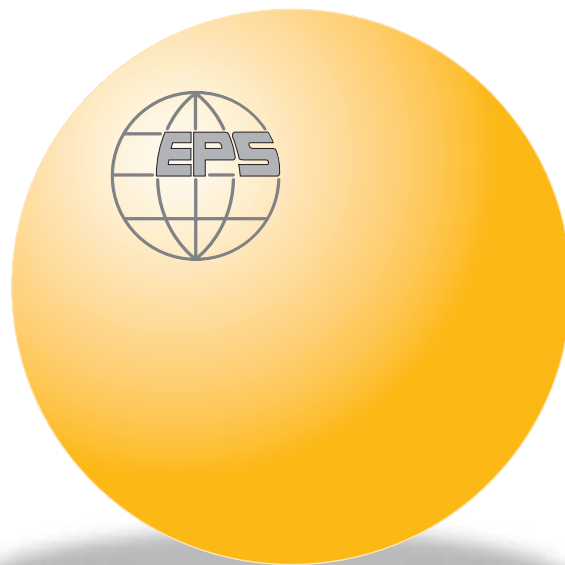
OFFPRINT

Vol. 69 • Number 3 • pp. 378–384

**Atomic clusters and phase transitions  
in the metastable  $\beta$ -Ta phase between 4.2 and 293 K**

\* \* \*

A. ARAKCHEEVA and G. CHAPUIS



Published under the scientific responsibility of the  
**EUROPEAN PHYSICAL SOCIETY**  
Incorporating  
JOURNAL DE PHYSIQUE LETTRES • LETTERE AL NUOVO CIMENTO



## Atomic clusters and phase transitions in the metastable $\beta$ -Ta phase between 4.2 and 293 K

A. ARAKCHEEVA and G. CHAPUIS

*Ecole Polytechnique Fédérale de Lausanne, Institut de Physique  
de la Matière Complexe - BSP, 1015 Lausanne, Switzerland*

received 19 July 2004; accepted in final form 19 November 2004

published online 5 January 2005

PACS. 61.50.-f – Crystalline state.

PACS. 61.66.Bi – Elemental solids.

PACS. 64.60.My – Metastable phases.

**Abstract.** – Atomic clusters were identified in the ground state of the non-equilibrium Ta phase (Frank-Kasper  $\sigma$ -structure type) at 15, 120 and 293 K. The evolution of the clusters with temperature leads to two phase transformations at 65 and 150 K which are related to the electrical and magnetic properties. The magnetic phase transition at 65 K is associated with the magnetic symmetry group transformation  $P4'_2/mn'm$  ( $< 65$  K) to  $P4'$  ( $> 65$  K). It is shown that  $\beta$ -U is also a two-component composite containing similar clusters. The nature of the stabilisation of  $\beta$ -Ta at the cathode is discussed.

*Introduction.* – The study of temperature-pressure ( $P$ - $T$ ) induced transformations of non-equilibrium phases is a very challenging topic from the thermodynamical point of view, even for pure metals [1]. This is even more the case, if the metastable phase can only be obtained under special conditions, for instance by electrodeposition. In order to understand the nature of their stabilisation and transformation, structural data depending on some thermodynamic parameter(s) are required. The metastable  $\beta$ -Ta phase (Frank-Kasper  $\sigma$ -structure, fig. 1) perfectly illustrates the complexity of this topic. It is well known [2–4] that  $\beta$ -Ta can be obtained either by electrodeposition (fine grains) or by sputtering deposition techniques on thin films, both at the cathode. Some aspects of the stabilisation and physical properties of  $\beta$ -Ta thin films have recently been studied in view of the technologically important combination of high electrical resistivity, good adhesion and low chemical affinity of  $\beta$ -Ta [2]. Therefore, its investigation is also of practical importance. The necessity of precise structural information of  $\beta$ -Ta has been raised in all publications related to this structure [2, 3]. Our single-crystal study of  $\beta$ -Ta gave us a unique opportunity to obtain precise structural data at room temperature and below. The impurity-free quality of the crystal was checked by microprobe analysis and confirmed by high-resolution single-crystal diffraction at 293 and 120 K [4]. In [4], the self-hosting two-component (host (H) - guest (G), fig. 1) composite structure with indistinguishable lattice constants, but different space groups for the components, is characteristic of  $\beta$ -Ta. Based on the space groups of the components, it was shown that the phase transition 293 (RT-I modification)  $\rightarrow$  120 (LT-I modification)  $\rightarrow$  293 (RT-II modification) is reversible

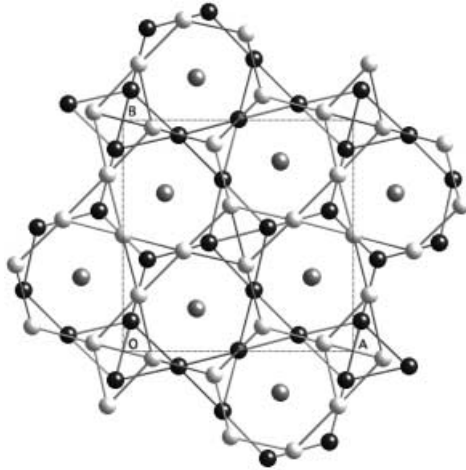


Fig. 1

Fig. 1 – A (001) projection of the tetragonal Frank-Kasper  $\sigma$ -structure type. Black and white spheres belong to the host (H) substructure, which consists of two H-nets located at  $z \approx 0.25$  (black), respectively,  $z \approx 0.75$  (white). Gray spheres ( $z \approx 0$  and  $0.5$ ) belong to the guest (G) substructure.

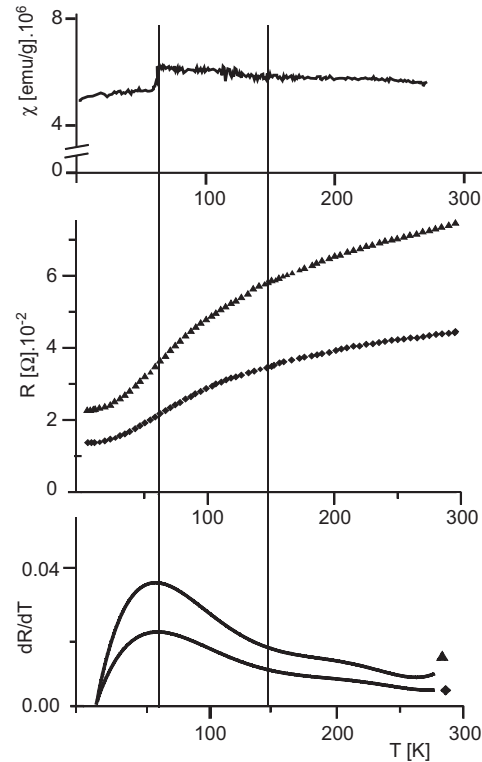


Fig. 2

Fig. 2 – Temperature dependences of the magnetic susceptibility  $\chi(T)$  (after [5]), the electrical resistance  $R(T)$  and the first derivative  $dR/dT$ . The  $R(T)$ -dependence was measured *in situ* for two polycrystalline bulks (cylindrical shape,  $2\text{-}3\text{ mm}^2$  in cross-section and  $2\text{-}3\text{ mm}$  in length) using the four-point probe technique (measuring current  $10^{-4}\text{ A}$ ). The characteristic temperatures of  $65$  and  $150\text{ K}$ , are indicated by vertical lines.

for H but irreversible for G. The  $\chi(T)$ -dependence measured on powder samples [5] indicates a magnetic phase transition at  $65\text{ K}$  (fig. 2). The non-linear dependence of the magnetization  $M(H)$  measured at  $77\text{ K}$  ( $1 < H < 4\text{ kOe}$ ) was satisfactorily approximated in [5] by assuming a contribution of the magnetic spin-spin interaction between atomic clusters possessing a localized charge, respectively, a magnetic moment:  $M(H) = M_0[\coth(m_{\text{cl}}H/T) - T/m_{\text{cl}}H]$ , where  $M_0 = Nm_{\text{cl}}$ . Moreover,  $M(H)$  is slightly non-linear at  $4.2\text{ K}$  [5]. However, these studies did not associate the concentration of the clusters,  $N \sim 10^{20}\text{ 1/mol}$ , and their magnetic moments,  $m_{\text{cl}} \sim 1000\ \mu_{\text{B}}$ , with any structural data.

The magnetic measurements triggered a new structural study of the same single crystal at helium temperature and the *in situ* measurement of the temperature dependence of the electrical resistance, which are reported here ( $R(T)$  in fig. 2). Only the most pertinent results of the LT-II ( $15\text{ K}$ ) structure are presented in this letter; all details on the refinement will be published elsewhere. The resistivity, as a characteristic of  $\beta\text{-Ta}$ , cannot be directly extracted from the  $R(T)$ -dependence (fig. 2). The important influence of the inter-grain boundaries of

the resistance should be accounted for in the fine-grain bulks. Indeed, two samples showed slightly different shape of the  $R(T)$  curve. Nevertheless, the first temperature derivative reveals common characteristic temperatures at 65 and 150 K, which correspond precisely to the  $\chi(T)$  curve (fig. 2). Both this result and the data obtained for the LT-II structure complete our previous studies [4, 5] and allow us to present here a more consistent interpretation of the low-temperature structure transformation.

In this letter, we report a new model of atomic cluster formation between 4.2 and 293 K and its evolution into the metastable  $\beta$ -Ta phase. We also report on the correlation between the type of clusters and the magnetic and electrical properties. The temperature-dependent evolution of the clusters is presented here with a new model of magnetic symmetry transformation of the commensurate composite structure for  $\beta$ -Ta. It is shown that the same composite characteristic and the temperature-dependent evolution of the clusters exist in another Frank-Kasper  $\sigma$ -structure, namely  $\beta$ -U.

*The nature of  $\beta$ -Ta stabilisation.* – It is most probable that the difficulty to obtain single crystals of  $\beta$ -Ta is directly linked to their stabilisation on the negatively charged surface of the cathode. This phase is brittle and shows a higher resistivity (150–220  $\mu\Omega\text{cm}$ ) in comparison to  $\alpha$ -Ta (15–30  $\mu\Omega\text{cm}$ ) [2]. In  $\beta$ -Ta, these properties point to a partial localization of electrons (PLE) in Ta-Ta bonds as opposed to metallic bonds in the bcc structure of  $\alpha$ -Ta. The PLE in metal-metal bonds is usually mediated by a high valence electron concentration (VEC). In all Frank-Kasper  $\sigma$ -structures (about 30 binary intermetallics and  $\beta$ -U) [6], the VEC is equal to 6–7  $e/\text{atom}$ , while metallic Ta contains only 5  $e/\text{atom}$ . We suggest that the high electron density on the cathode surface stimulates the increase of the VEC for Ta in the crystallisation, and its  $\sigma$ -structure type can only be stabilised as *negatively charged* crystallisation nuclei. The crystals can grow as neutral thin film or fine grains owing to a stabilisation by interface energy. Our experience confirms this observation: a small (20  $\mu$ ) crystal of  $\beta$ -Ta was isolated by mechanical splitting of a two-phase specimen (50  $\mu$ ). Hence, a precise single-crystal structure investigation of  $\beta$ -Ta was possible owing to the rare case of an extended interface between two different single crystals. This pure and unique crystal was used for X-ray diffraction experiments with the following temperature changes: 293  $\rightarrow$  120  $\rightarrow$  293  $\rightarrow$  15 K.

The impurity effect is discussed [2] as a possible reason for the formation of  $\beta$ -Ta. Our study leaves room for a possible VEC increase due to impurity. However, the stabilisation of  $\beta$ -Ta by impurity would favor its formation in some neutral environment, which is apparently not the case.

*Electrical and magnetic properties of  $\beta$ -Ta and the formation of clusters.* – The term cluster implies the formation of a group of atoms with interatomic distances essentially shorter (4–7 per cents) than between groups. The decrease of some Ta-Ta distances in  $\beta$ -Ta, compared to the metallic bond length of 2.86 Å in  $\alpha$ -Ta, is not surprising, owing to the partial localization of electrons in the Ta-Ta bonds mentioned above. Indeed, a careful analysis of the bond lengths based on the high-resolution structure refinement [4] and the present work clearly reveals the formation of clusters.

The histogram of the Ta-Ta bond lengths calculated for 293, 120 and 15 K is represented in fig. 3. Considering that the metallic bond is  $2.86 \pm 0.05$  Å, values shorter than 2.81 Å are characteristic of cluster bonds.

As illustrated in fig. 3, the G(uest) substructure consists only of the shortest cluster bonds, ( $\sim 2.65$  Å) at all temperatures. All G atoms are indeed associated to one-dimensional atomic clusters, the G-chains, which are located in the channels formed by the H(ost) substructure normal to the H-nets (fig. 1). The G-chains are temperature independent in the sequence 293-120-15 K. The other cluster bonds are confined in the H-net plane (fig. 4). In the lowest-

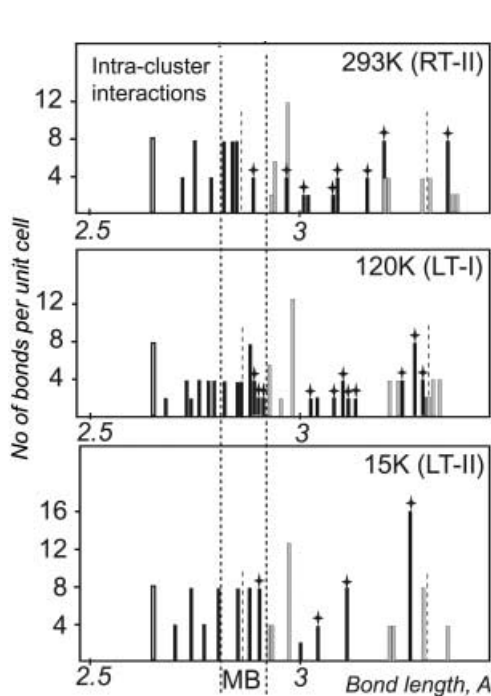


Fig. 3

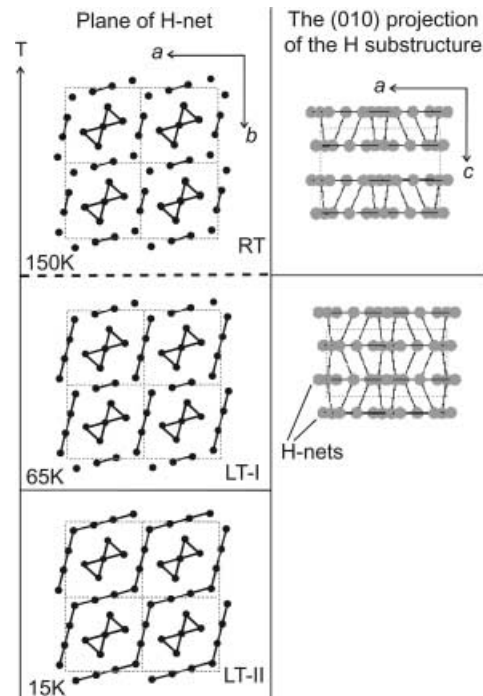


Fig. 4

Fig. 3 – Histograms of Ta-Ta bond lengths calculated for the RT-I, RT-II, LT-I and LT-II modifications of  $\beta$ -Ta. The bonds within the H substructure, the G substructure and between them are shown with black, white, respectively, gray colors. The bonds between H-nets are indicated with stars in order to single them out. The dashed lines indicate the bond lengths 2.86 and 3.30 Å observed in  $\alpha$ -Ta. The dotted lines show the conventional boundaries (2.81, 2.91 Å) of metallic bonds (MB).

Fig. 4 – Schematic representation of the temperature-dependent evolution of the H substructure of  $\beta$ -Ta. The short intra-cluster bonds are indicated by bold lines. The metallic inter-cluster bonds connecting the H-nets are indicated by thin lines. The dashed lines indicate the unit cells.

temperature modification, every H-net consists of infinite one-dimensional clusters of zigzag H-chains, which are separated by five atom clusters forming a butterfly (fig. 4). Among all the clusters, only the H-chains are temperature dependent. With increasing temperature, they progressively evolve into clusters of atomic pairs at RT.

The continuous array of metallic bonds linking the H-nets along  $c$ , at both 120 and 15 K (fig. 4), is absent at 293 K. At this temperature, the H-nets are forming pairs with distances about 2.885 Å. The shortest bond linking pairs, 2.97 Å, is significantly longer. At 120 and 15 K, some metallic bonds in the range 2.89 to 2.91 Å are randomly distributed between the H-nets along  $c$  (fig. 4). The weaker interactions between the H-nets as well as between the H and G substructures exhibit interatomic distances longer than 2.92 Å. Distances longer than 3.28 Å (fig. 3) represent the weakest inter-chain interactions in the structure.

Taking into account the existence of clusters and the  $dR/dT$  (fig. 2) dependence, our analysis allows to draw the following conclusions illustrated in (fig. 4).

- 1) In the 150–293 K range, the nearly constant value of  $\chi(T)$  (fig. 2) is associated with a stable cluster structure characteristic of the RT modifications.
- 2) In the 65–150 K range, the infinite array of metallic bonds linking the H-nets gives

TABLE I – Evolution of the space and magnetic group symmetry of  $\beta$ -Ta at various steps of the thermal history 293  $\rightarrow$  120  $\rightarrow$  293  $\rightarrow$  15 K.

$T$ , K (phase notation; type of structure)	$a$ , $c$ unit cell parameters, Å	Space (magnetic) groups of substructures: H; G
293 (RT-I; non-composite)	10.211(3), 5.3064(10)	Both: $P\bar{4}2_1m$ ( $P\bar{4}'2'_1m$ <sup>a</sup> )
120 (LT-I; composite)	10.1815(5), 5.2950(1)	$P\bar{4}$ ( $P\bar{4}'$ ); $P4/mbm$ ( $P4'/mb'm$ <sup>a</sup> ) <sup>b</sup>
293 (RT-II; composite)	10.201(1), 5.3075(5)	$P\bar{4}2_1m$ ( $P\bar{4}'2'_1m$ <sup>a</sup> ); $P4/mbm$ ( $P4'/mb'm$ <sup>a</sup> ) <sup>b</sup>
15 (LT-II; composite)	10.167(3), 5.295(1)	$P4_2/mnm$ ( $P4'_2/mn'm$ ); $P4/mbm$ ( $P4'/mb'm$ ) <sup>b</sup>

<sup>a</sup> The most probable magnetic group (see the text and fig. 6); <sup>b</sup>  $c_G = 0.5 c_H$ .

rise to changes in the  $dR/dT$  curve as compared to the 150–293 K range. Different combinations of discrete clusters are possible within the zigzag H-chains. The average number of atoms per cluster increases continuously by decreasing temperature. This is associated to a continuous increase of  $\chi(T)$ .

- 3) Below 65 K, the stabilisation of the infinite zigzag H-chains relates to the flattening of  $R(T)$ . In addition, the transformation from the discrete clusters in the H-chains into infinite clusters is associated with a sharp decrease of  $\chi(T)$  at 65 K.

*The symmetry of the commensurate composite structure  $\beta$ -Ta.* – At low temperature, the evolution of the  $\beta$ -Ta clusters occurs as expected, *i.e.* the number of shorter distances increases with decreasing temperature. However, the structure transformation shows an unexpected symmetry transformation. Table I shows the evolution of the structure symmetry with the thermal history 293 (RT-I)  $\rightarrow$  120 (LT-I)  $\rightarrow$  293 (RT-II)  $\rightarrow$  15 (LT-II) K. As indicated in [4] for the RT-II and LT-I modifications, the symmetry is characterized by three space groups: one for the H substructure, one for the G substructure and one for the (H+G) combination. The symmetry of the LT-II modification confirms and reinforces this conclusion. After an initial cooling from 293 to 120 K, the structure transformed irreversibly from the non-composite RT-I state (a common space group describing both H and G substructures) to a two-component composite state (the space group of G is a supergroup of H). Following a further thermal treatment including heating and cooling, the G substructure maintains both symmetry and structure (interatomic distances), while the H substructure changes both its symmetry (table I) and cluster structure (fig. 4). The composite modifications are characterized by weak interactions between H and G (fig. 3). No experimental evidence pointing to an incommensurate phase was observed in our experiments. Therefore, this two-component composite is commensurate.

*$\beta$ -U, another example of Frank-Kasper  $\sigma$ -structure containing atomic clusters.* – We postulate that every Frank-Kasper  $\sigma$ -structure tends to have a two-component composite structure (commensurate or incommensurate) under some specific  $P$ - $T$  conditions. For instance, our brief analysis of the  $\beta$ -U interatomic distances based on structural data obtained at 955, 973 and 1030 K [7] indicates important similarities with  $\beta$ -Ta. The unusually short U-U bonds observed in the G-chains and in the plane of the H-net give rise to the formation of clusters. This distance can be compared to the metallic bond, 3.06 Å, observed in the bcc  $\gamma$ -U structure [6]. However, in contrast to  $\beta$ -Ta, the G-chains of  $\beta$ -U are temperature dependent, whereas the H substructure is not (fig. 5). In the G-chain, different neighboring U-U distances are observed at 955 (2.89(1), respectively, 2.76(1) Å) and at 973 K (2.92(1), respectively, 2.74(1) Å). Both types of short bonds exist in low-temperature  $\alpha$ -U (2.75 and

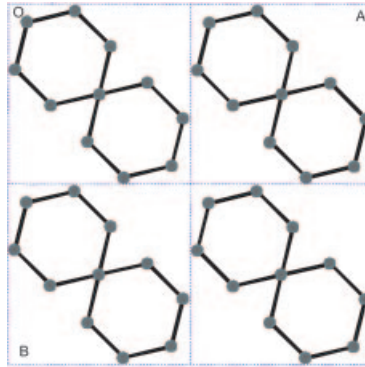


Fig. 5 – The cluster structure of the  $\beta$ -U H-net. The intra-cluster bonds connecting U atoms (gray spheres) with distances 2.90–2.98(1) Å are indicated by bold lines. The inter-cluster atomic distances, 3.02–3.13 Å, are metallic bonds; they are close to 3.06 Å in  $\gamma$ -U. Interatomic distances between H-nets fall into the 3.20–3.55 Å range. These values correspond to the long U-U distances 3.27 and 3.45 Å in  $\alpha$ -U. All distances in the H substructure vary within 0.5–1 standard deviation in the temperature range 955–1030 K.

2.86 Å [6]). At 1030 K, the difference between the bonds in the G-chain disappears as well as the shortest U-U distances: the bond lengths 2.85(3) and 2.81(3) Å are equal within one standard deviation. This transformation is perhaps associated to a phase transition between 973 and 1030 K. At 1030 K,  $\beta$ -U can be described with the same composite symmetry as  $\beta$ -Ta at 15 K (table I). Experimental powder diffraction data of  $\beta$ -U [7] cannot exclude a possible incommensurate structure. Therefore at 1030 K [7],  $\beta$ -U is a commensurate or incommensurate two-component composite similar to  $\beta$ -Ta.

*Temperature dependence of the magnetic symmetry of  $\beta$ -Ta.* – Taking into account the contribution of the spin-spin interactions between magnetic moments of charges localized on the clusters owing to PLE on each single intra-cluster bond [5], the magnetic space groups can be related to the corresponding symmetry of  $\beta$ -Ta. In particular, the magnetic group of G should be a supergroup of H at the same temperature and should allow the existence of some clusters with opposite spins at the corresponding temperatures. The composite magnetic symmetry (H and (H + G):  $P4'_2/mn'm$ ; G:  $P4'/mb'm$  ( $c_G = 0.5c_H$ )) is only possible at 4.2 K, *i.e.* below 65 K. Six other magnetic groups from the  $P4_2/mnm$  family do not allow opposite spins

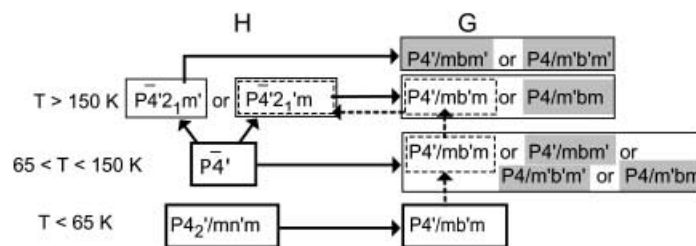


Fig. 6 – The logical scheme of the magnetic symmetry identification. The unambiguous magnetic groups are indicated in solid frames. The bold arrows show certain correlations between groups. The dashed arrows show the most probable correlations, and the most probable groups are enclosed in dashed frames. Gray rectangles mark the “black-and-white” magnetic groups, which are “gray” for the G component owing to special atomic sites.



in the H clusters and  $P4'/mb'm$  is the only magnetic supergroup of H. The magnetic symmetry  $P\bar{4}'$  of H and (H+G) is only possible in the 65–150 K range. (The atlas of black-and-white space group [8] was used for the magnetic space groups identification.) The unequivocal identification of other magnetic groups is not possible on the basis of the present data. However, assuming a stable magnetic structure G, the most probable magnetic space groups have been identified (fig. 6) for both H and G components at every temperature (table I). As could be extracted from table I, the magnetic phase transition of  $\beta$ -Ta at 65 K corresponds to the magnetic group transformation of the H component from  $P\bar{4}'$  to  $P4'_2/mn'm$ . Since the zigzag H-chains are the only temperature-dependent structural units, it is logical to propose that this phase transition is specifically related to spin-spin interactions within the H-chains. Indeed, below 65 K, in the magnetic group  $P4'_2/mn'm$ , all infinite H-chains located within one H-net exhibit the same magnetic spin. Above 65 K, in the magnetic group  $P\bar{4}'$ , at least two independent clusters exist in each H-net. Therefore, two orientations of magnetic spin of the clusters can exist within the same H-net. Hence, the magnetic phase transition below 65 K can be associated to the stabilisation of the single spin orientation for all H-chains within each H-net.

The unusually low concentration of clusters (1 cluster per 200 unit cell) and large magnetic moment ( $1000 \mu_B$ ) of each cluster as obtained in [5] at 77 K can now be explained with the cluster model introduced in this study. Indeed, the length of the cluster is extending over many cells when the temperature approaches 65 K, temperature at which the cluster reaches an infinite length. The long cluster can have a large magnetic moment owing to the large number of short intra-cluster bonds.

\* \* \*

This work is supported by the Swiss National Science Foundation, grant No. 2067698.02 and partially by the Russian Foundation for Basic Research (grant 02-03-32982). The contributions of H. ZÚÑIGA and V. PETRIČEK are gratefully acknowledged.

#### REFERENCES

- [1] BARICCO M., *Key Eng. Mat.*, **103** (1995) 1; TOURNIER S., BARTH M., HERLACH D. M. and VINET B., *Acta Mater.*, **45** (1997) 191; CLAVAGUERA-MORA M. T., *Termochim. Acta*, **314** (1998) 281.
- [2] LEE S. L. *et al.*, *Surf. Coatings Technol.*, **177-178** (2004) 44; KLAVER P. and THIJSSSE B., *Thin Solid Films*, **413** (2002) 110; WHITACRE J. F. and BILELLO J. C., *J. Vac. Sci. Technol. A*, **19** (2001) 2910; JIANG A. *et al.*, *Thin Solid Films*, **437** (2003) 116; STAVREV M. *et al.*, *Thin Solid Films*, **307** (1997) 79.
- [3] MOSELEY P. T. and SEABOOK C. J., *Acta Crystallogr., Sect. B*, **29** (1973) 1170; YOUNG D. A., *Phase Diagrams of the Elements* (University of California Press, Berkeley) 1991.
- [4] ARAKCHEEVA A., CHAPUIS G. and GRINEVITCH V., *Acta Crystallogr., Sect. B*, **58** (2002) 1; ARAKCHEEVA A. *et al.*, *Acta Crystallogr., Sect. B*, **59** (2003) 324.
- [5] SHAMRAY V. F., WARHULSKA J. K., ARAKCHEEVA A. V. and GRINEVITCH V. V., *Crystallogr. Rep.*, **49** (2004) 930.
- [6] PEARSON W. B., *The Crystal Chemistry and Physics of Metals and Alloys* (Wiley, New York) 1972.
- [7] LAWSON A. C. and OLSEN C. E., *Acta Crystallogr., Sect. B*, **44** (1988) 89.
- [8] KOPTSIK V. A., *Shubnikov Groups. Handbook of Symmetry and Physical Properties of Crystal Structures* (Moscow State University, Moscow) 1966.